CONCRETE LIBRARY OF JSCE NO. 5, AUGUST 1985

EXPERIMENTAL STUDIES ON SHEAR STRENGTH OF LARGE REINFORCED CONCRETE BEAMS UNDER UNIFORMLY DISTRIBUTED LOAD

(Translation from Proceeding of JSCE, No. 345/V-1, August 1984)

Mizuhito IGURO

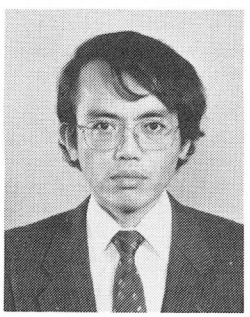

Toshiyuki SHIOYA

Yoichi NOJIRI

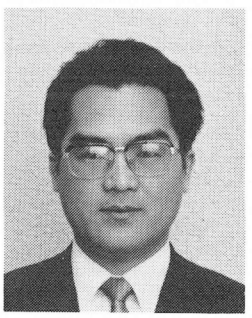

Hikaru AKIYAMA

SYNOPSIS

In the past, several researchers have studied the size effect on shear strength of reinforced concrete beams and it has been found that the nominal shear strength V_c/bd of beams without shear reinforcement decreases as the effective depth of member increases. However, effective depths in previous studies were limited to only 110 cm. In order to investigate the size effect for larger reinforced concrete members, this study was undertaken on members with six different depths ranging from 10 to 300 cm, with constant b/d ratio, under uniformly distributed loads. The results reveal that the size effect exists even for a member deeper than 100 cm, and the nominal shear strength is inversely proportional to the fourth root of the effective depth.

M. Iguro, General Manager, Civil Engineering Development Department, Shimizu Construction Co., Ltd., Tokyo, Japan. He is a member of JSCE and JCI.

T. Shioya, Research engineer, Institute of Technology, Shimizu Construction Co., Ltd., Tokyo, Japan. He is a member of JSCE and JCI.

Y. Nojiri, General Manager, Civil Engineering Department, Kajima Institute of Construction Technology, Tokyo, Japan. He is a member of JSCE and JCI.

H. Akiyama, Senior research engineer, Kajima Institute of Construction Technology, Tokyo, Japan. He is a member of JSCE and JCI.

1. INTRODUCTION

In recent years, reinforced concrete structures are showing a gradual trend to become larger in size as advances and improvement are made in materials, design and construction technologies, and also because of the demands of society. One of the problems in design accompanying increased size is the matter of how to design against shear. Studies on reinforced concrete members are going on actively even now, and much work has also been done regarding shear strength, but the present situation is that any universally recognized method of design does not exist. The usual practice in the standard of each country is to use experimental formulae derived from statistical data in experiments or to prescribe allowable values based on test results.

In designing a larger-sized structure, the design against shear is also done referring to these experimental formulae and allowable values. The shear strength of a reinforced concrete beam without shear reinforcement has been shown by experimental research done by Kani [1], Kennedy [2], Taylor [3] and others where shear strength is reduced with increased effective depth "d", as shown in Fig. 1. This is generally called the "size effect," and has been taken up in specifications such as the CEB-FIP "Model Code for Concrete Structures" [4], and the Japan Society of Civil Engineers (JSCE) "Limit State Design of Concrete Structures (Proposal)" [5] and others. However, there are no reports on the size effect on reinforced concrete beams of d > 110 cm. Furthermore, there have been difficulties in assessing the shear capacity of a large structural member, which is subjected to large dead weight uniformly distributed load, due to lack of the experimental data on the effect of this distributed load, since almost all experiments in the past were performed under concentrated loads. Because of this, experiments under uniformly distributed loads on reinforced concrete beams of d = 10 to 300 cm without shear reinforcement were conducted with an attempt made mainly to grasp the existence and extent of the size effect on shear strength of beams of d > 100 cm.

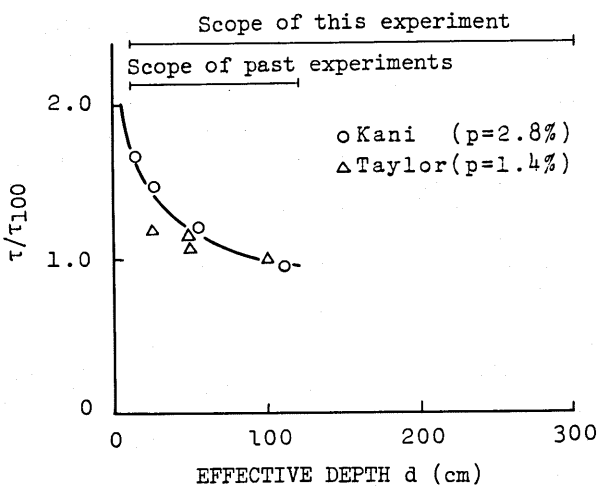

Fig. 1 Relation of shear strength "τ" and effective depth "d" (where τ_{100}: shear strength of beam with effective depth d = 100 cm)

2. OUTLINE OF EXPERIMENTS

The specimens listed in Table 1 were made under the following conditions :

(1) Six effective depths "d" of specimens are chosen as 10, 20, 60, 100, 200 and 300 cm.
(2) The applied load is to be a uniformly distributed load.
(3) The maximum size of coarse aggregate Gmax is to be Gmax = 10 mm in case of $d \leqq 100$ cm and Gmax = 25 mm in case of $d \geqq 100$ cm, and the effect of coarse aggregate size to shear strength is investigated by beams of d = 100 cm.
(4) The principal configuration of the specimen is to be a beam of rectangular cross section and the ratio of width of specimen "b" to "d" is to be b/d = 1/2.
(5) The ratio of loading span "ℓ" to "d" is to be ℓ/d = 12. In case of concentrated load, the ratio of shear span "a" to "d" for diagonal tension failure will be $a/d \geqq 3$ as shown in Fig. 2, while according to Kani [7], the shear span "a" in case of uniformly distributed load will be $a = \ell/4$ as shown in Fig. 3. Consequently, with $\ell/d \geqq 12$, there will be diagonal tension failure and the resisting mechanism will not be of deep beam, and therefore, ℓ/d = 12 was adopted. The ratio will give a value close to the lower limit of shear strength.
(6) The main reinforcement ratio "p" in the vicinity of the supporting point where shear failure would occur is taken to be 0.4 percent. The occurrence of shear failure in a reinforced concrete member will be more likely in case larger "p" is adopted, but here p = 0.4% was taken as being a reinforcement ratio close to the lower limit being actually used, thereby obtaining the lower limit value of shear strength.
(7) Reinforcing bar diameter is to be varied in proportion to effective depth.

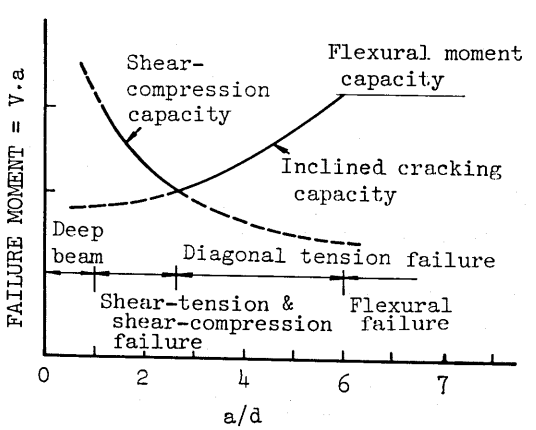

Fig. 2 a/d and shear strength [6].

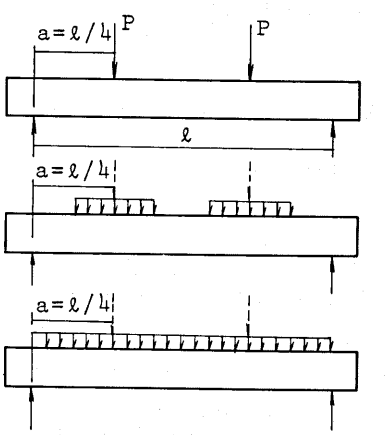

Fig. 3 Shear span ratio in case of a uniformly distributed load.

2.1 Configurations, Dimensions and Reinforcing Bar Arrangements

The cross-sectional dimensions of the specimens and the reinforcing bar arrangements in the vicinities of the supporting points are shown in Fig. 4. The specimens of effective depths d = 200 cm and 300 cm were made with constant reinforcement ratio of 0.4 percent, but for specimens of d ≦ 100 cm, since it was expected that flexural failure at midspan would precede shear failure, the portion from 1.5 d from supporting point to midspan was reinforced against flexure. The quantity of reinforcement was increased by increments of 0.05 percent at a pitch of 0.25 from 1.5 d to 3 d, while from 3 d to midspan a constant ratio of 0.8 percent was adopted.

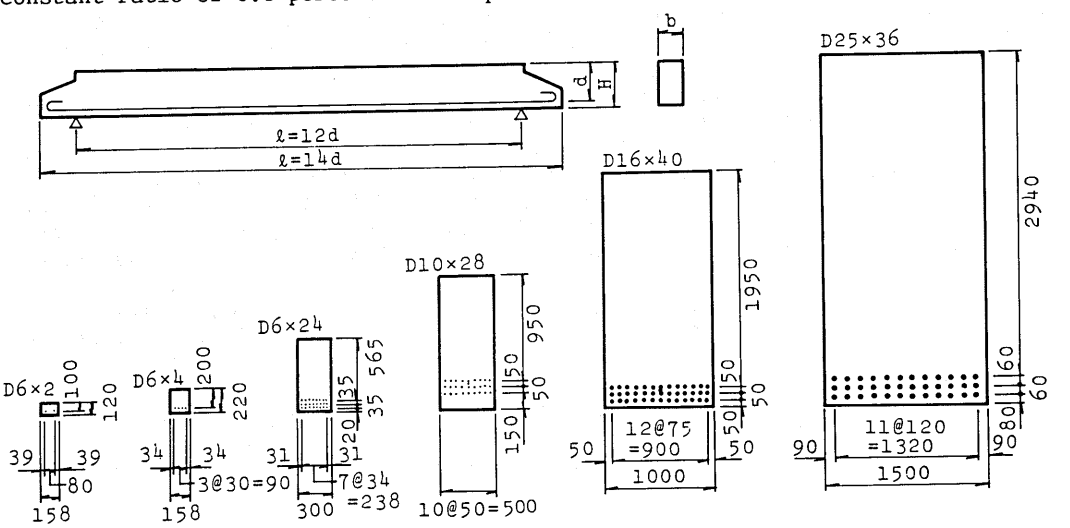

Fig.4 Cross-sectional dimensions and reinforcing bar arrangements of specimen.

2.2 Materials Used

a) Concrete

The mix proportions of concrete are shown in Table 2.

b) Reinforcing Bar

The reinforcing bars used were D3, D6, D10, D16 and D25. The yield points of the respective bars are shown in Table 1. The bond surface deformations of the reinforcing bars were of wave lugs for D6 and bamboo lugs for others. Reinforcing bars of D3 [8] were used only for reinforcement against flexure.

Table 2 Mix proportions

Mix	Comp. strength fc (MPa)	Max. size coarse agg. (mm)	Range of slump (cm)	Water-cement ratio W/C	Sand-agg. ratio S/a	Unit content (m^3) Water W (kg)	Cement C (kg)	Sand S (kg)	Gravel G (kg)	Admixture (cc/m^3)	Air (%)
1	23.5	10	15 ± 2	0.615	50	176	287	915	927	718	4
2	23.5	25	12 ± 2	0.560	41.5	149	266	785	1123	669	4

Table 1 Varieties of specimens and principal test results

Specimen No.	Specimen dimensions						Concrete				Reinforcing bar		Reinforcement ratio		Failure load	Shear stress acting at failure		Failure mode	Loading from
	Effective depth	Loading span	Loading span ratio	Length	Heigth	Width	Max. size coarse agg.	Age at test	Comp. strength	Tensile strength	Dia.	Yield point	Axial direction			Evaluated at 1.5 d location from supporting point			Top / Bottom
													Supporting point to 1.5d location	Midspan					
	d (cm)	ℓ (cm)	ℓ/d	L (cm)	H (cm)	b (cm)	G_{max} (mm)	(day)	(MPa)	(MPa)	D	fsy (MPa)	pr1 (%)	pr2 (%)	qu (MPa)	τ_u** (MPa)	τ_{uc}*** (MPa)		
1	10	120	12	140	12	15.8	10 (Mix 1)	48	20.6	1.85	(D3)* D6	(320)* 440	0.4	0.8	0.186	(0.837)	(0.875)	Flexural failure	Top
2	20	240	12	280	22	15.8	10 (Mix 1)	44	19.7	1.87	(D3) D6	(320) 440	0.4	0.8	0.187	(0.843)	(0.894)	Flexural failure	Top
3	60	720	12	840	65.5	30	10 (Mix 1)	28	21.1	1.81	(D3) D6	(440) 440	0.4	0.8	0.103	0.464	0.481	Diagonal tension failure	Top
4	100	1200	12	1400	120	50	10 (Mix 1)	42	27.2	2.05	(D10) D10	(370) 370	0.4	0.8	0.079	0.356	0.339	Diagonal tension failure	Top
5	100	1200	12	1400	120	50	25 (Mix 2)	41	21.9	2.23	(D10) D10	(370) 370	0.4	0.8	0.088	0.397	0.407	Diagonal tension failure	Top
6	200	2400	12	2800	210	100	25 (Mix 2)	35	28.5	2.73	D16	370	0.4	0.4	0.077	0.349	0.327	Diagonal tension failure	Bottom
7	300	3600	12	4200	314	150	25 (Mix 2)	35	24.3	2.19	D25	360	0.4	0.4	0.070	0.314	0.311	Diagonal tension failure	Bottom

* Reinforcing bar used against flexure

** $\tau_u = V_c/bd = q_u \times 4.5$

*** Corrected value according to compressive strength $\tau_{uc} = \tau_u \times (23.5/f_c)^{1/3}$

2.3 Placing and Curing of Concrete

The concrete of large specimens of d = 200 cm, 300 cm were placed by pump. The specimens were cast divided into multiple layers with a single layer approximately 80 cm and the rate of placement 50 cm/hr. Consequently, in case of d = 300 cm the specimen was divided into four layers with 1.5 hrs required per layer, so that it took approximately 6 hrs to cast the specimen. Test pieces for quality control were made using concrete sampled after discharge from the pump. Specimens except large ones were cast by chutes. Specimens were cured by sprinkling water from immediately after placement until the age of 28 days.

2.4 Method of Test

The supporting condition for beams was simple supports at both ends, and the uniform load was applied to a beam using a synthetic-rubber bag which exerts uniform hydraulic pressure based on Pascal's Law. The loading apparatus used in case of the largest specimen is shown in Fig. 5. A uniformly distributed load acting on the specimen with this method was confirmed in preliminary tests using the pressure sensitive film. During actual tests, loads were measured by two systems of pressure gauges and load cells. The pressure assured that the specified loads were acting.

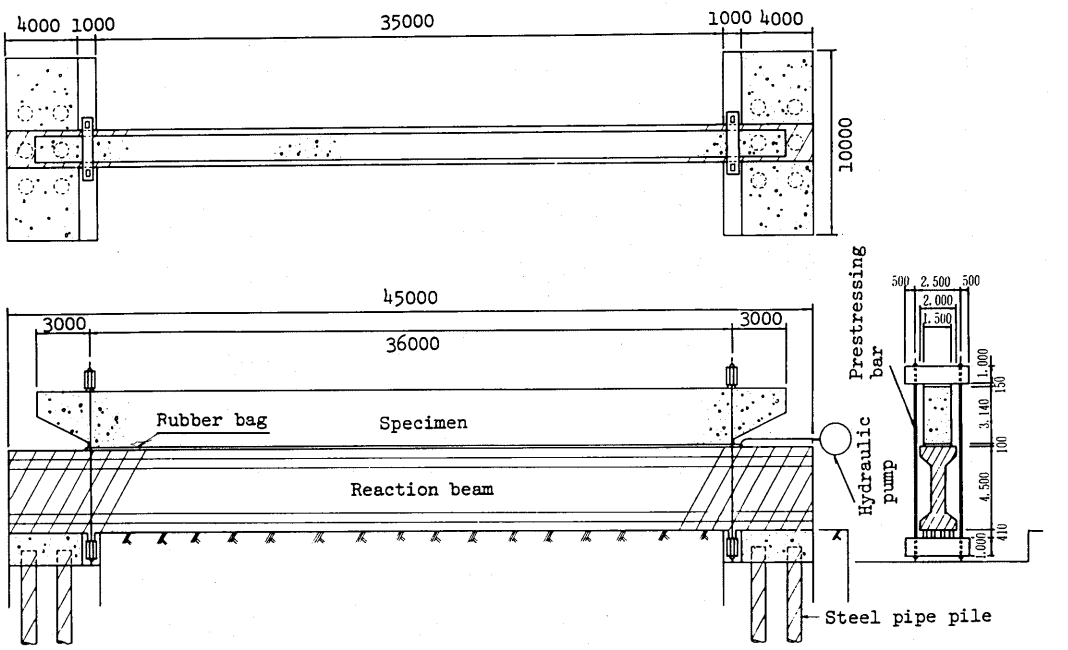

Fig. 5 Loading apparatus for the largest beam.

With regard to handling of dead weight, in case of loading from the top, the dead weight was measured by load cells and converted to a uniformly distributed load and added to the applied load. In case of loading from the bottom, the condition of the specimen floating on a synthetic-rubber bag filled with water was taken to be zero loading. The cycles of loading were given as described below.

a) First Cycle

Up to the load at which extreme fiber stress of the specimen reaches tensile strength of concrete.

b) Second Cycle

Up to the load at which shear stress acting on the cross section at 1.5 d inside from a supporting point reaches the allowable value τ_{a1} for a beam according to the current Japan Society of Civil Engineers Standard Specifications for Unreinforced and Reinforced Concrete [9]. In this specification shear stress is defined as $\tau = V_c/bjd$, but in this study shear stress is evaluated as $\tau = V_c/bd$. Consequently, τ_{a1} = 0.38 MPa in this study corresponds to τ_{a1} = 0.44 MPa in case of f_c =23.5 MPa in the specification.

c) Third Cycle

Up to failure load.

2.5 Additional Tests

The following tests were performed on large specimens with the purpose of investigating the factors causing the size effect on shear strength of reinforced concrete members.

a) Bond Strength Tests of Reinforcing Bars

The method of testing bond strength for the case of d = 300 cm is shown in Fig. 6. This method was also followed in the case of d = 200 cm. In the specimen of

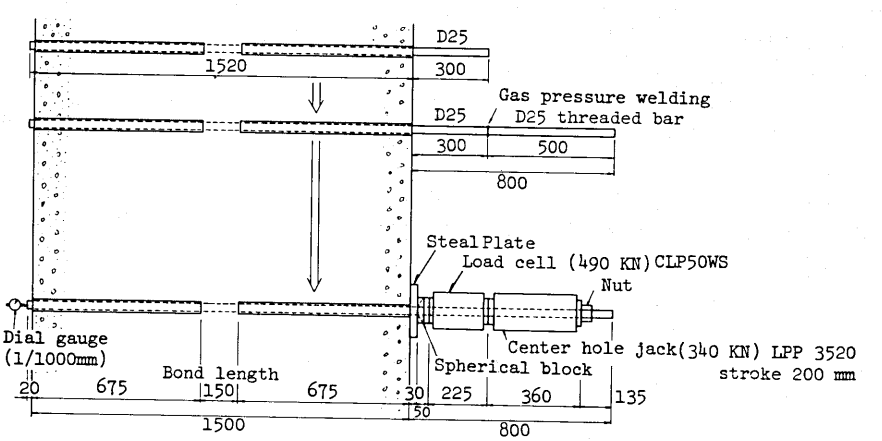

Fig. 6 Bond strength test (Specimen No.7)

d = 300 cm, the reinforcing bars used were D25 with the bond lengths of 15 cm at the middle, the remainders being unbonded. The pull out test was conducted using a center hole jack and measurements were taken until movement of the free end of a bar reached 1 mm. The locations of bars for bond strength tests are shown in Fig. 7 for the case of d = 300 cm. The locations were determined similarly in case of d = 200 cm.

b) Concrete Core Strength Tests

Core strength tests were performed on specimens of d = 200 cm and 300 cm. The locations of core sampling for compressive strength tests are shown in Fig. 7.

2.6 Items of Measurement

The items of measurement and specifications of instruments are shown in Table 3.

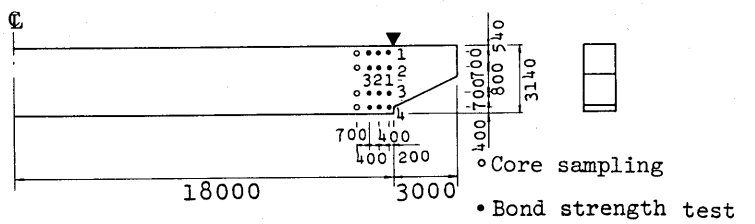

Fig. 7 Location of bars for bond strength test and core sampling (Specimen No.7)

Table 3 Items of measurement and specifications of instruments

Masurement item	Measurement objective	Measurement method	Instrument specifications	N*	Remarks
Load applied	Confirmation of strength	Load cell	Capacity (980- 5900 KN)	1 or 2	
Pressure applied	Ditto	Pressure gauge	Capacity (0.2- 0.5 MPa)	2	
Concrete strain	Confirmation of failure mode	Strain gauge	PL-60 or KM 100F	10	19 points for specimens of d = 200, 300 cm
Rebar strain	Ditto	Ditto	FLA-6-11 or FCA-6-11	10	Ditto
Deflection	Ditto	Displacement meter	CDP-50 or VPS	15	
Crack distribution	Ditto	Visual inspection	-	-	
Crack width	Ditto	Displacement meter	CE-5, PI-5 or crack scale	8	
Failure mode	Ditto	Visual inspection	-	-	

* Number of measurement points

3. EXPERIMENTAL RESULTS AND OBSERVATIONS

The experimental results are as shown in Table 1. Since there was a slight difference in concrete strength of specimens tested at different ages as shown in Table 1, the correction was made on the shear strength by a normalizing factor, by which the measured shear strength was made proportional to the cubic root of the measured compressive strength [10]. These corrected values were used in the subsequent studies. Furthermore, in case of a uniformly distributed load, shear force distribution is not constant along shear span as in the case of concentrated load, and the distribution will be linear decrease toward the midspan as shown in Fig. 8. Consequently, the shear strength $\tau = V_c/bd$ differs along the span, and in this study the section at 1.5 d inside from a supporting point was assumed to be the critical section referring to cracking patterns.

3.1 Evaluation of Size Effect

Figure 9 shows the results of these experiments with the calculated values of shear strength applying established standards and Okamura-Higai equation [10]. According to these results, the shear strength is gradually reduced as effective depth increases, similarly to the results of studies by Kani and Taylor. Furthermore, although the CEB/FIP "Model Code for Concrete Structures" does not

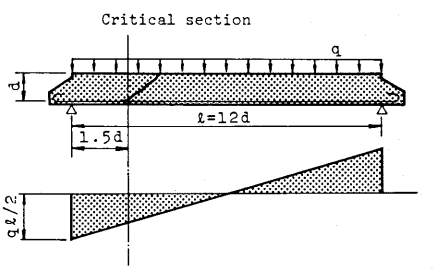

Fig. 8 Shear force diagram and critical section.

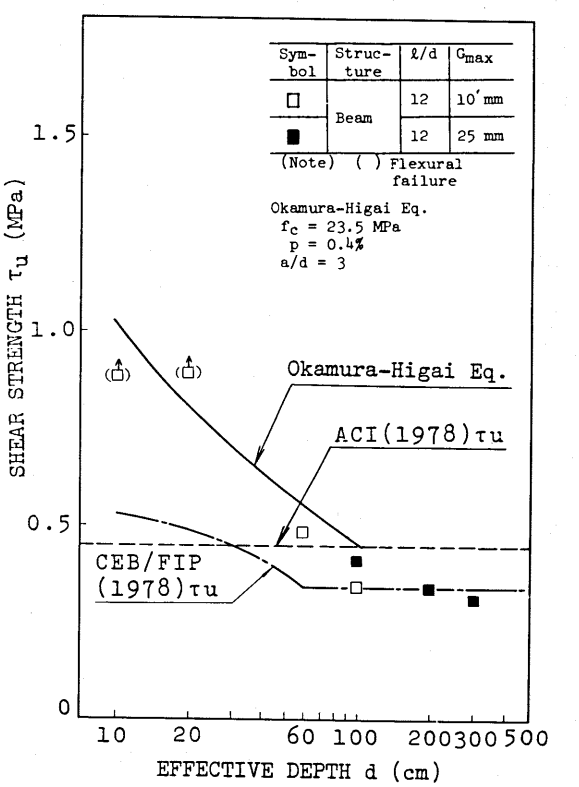

Fig. 9 Shear strength and effective depth
-- evaluated at 1.5d from supporting point
-- correction by compressive strength

take the size effect for consideration at d > 60 cm, the size effect still exists even for d > 100 cm which is outside the scope of the past experiments. Particularly, in case of a specimen of d = 300 cm and main reinforcement ratio of 0.4 percent without shear reinforcement, the shear strength was τ_u = 0.31 MPa, that indicates a fairly small value. The shear strength equation by Okamura and Higai adopted in the JSCE "Limit State Design of Concrete Structures (Proposal)" was derived from the experimental results on shear strength under concentrated loads. The data were collected from a number of Japanese and foreign literatures. Even in case of a uniformly distributed load as in our experiments, there is approximate compliance with the equation in the range of d < 100 cm if evaluation is made with a/d = ℓ/4d. Figure 10 shows the relation of effective depth and shear strength plotted on logarithmic paper with the shear strength $\tau_{100.25}$ (d = 100 cm and Gmax = 25 mm) as a reference in order to see the size effect. According to the results of experiments, the size effect shows a slight convex trend in the downward direction. Although it does seem that a lower limit exists at around d = 200 to 300 cm, because of a little amount of experimental data available it appears advisable in the present stage to consider that the shear strength is inversely proportional to the fourth root of effective depth as shown by the solid line in the figure.

Furthermore, the effect of the size of coarse aggregate (Gmax) was investigated using d = 100 cm beams, and the shear strength of a beam with Gmax = 25 mm was higher about 20% than that of Gmax = 10 mm.

As described above, it was found that there is the size effect on shear strength even with d > 100 cm beams. Therefore, in subsequent studies, the behaviors of specimens with d = 300 cm are described in detail, and the factors causing the size effect are examined.

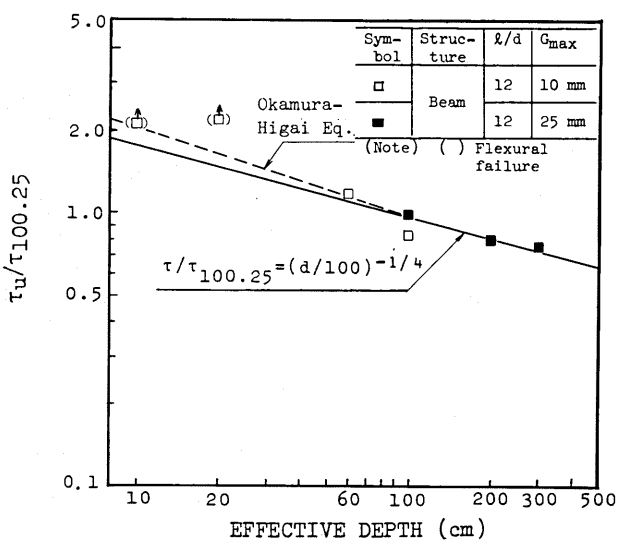

Fig. 10 Shear strength ratio and effective depth.

3.2 Cracking Patterns

The cracking patterns of the various specimens are shown in Fig. 11. Flexural cracks occurred at extreme tension fiber of the midspan in all specimens, and when loads were increased, cracks already formed propagated to extreme compression fiber, while newly formed flexural cracks were observed from midspan to shear spans. With the specimens of d = 10 and 20 cm, flexural failures occurred at the midspan before shear failures occurred, but with specimens of d $\geqq$ 60 cm, diagonal cracks produced in the vicinities of 1.5 d from the supporting points became more dominant than flexural cracks at the midspan. Finally, sudden failure occurred at shear span. Specimens of d $\geqq$ 60 cm showed diagonal tension failures, but the cracking patterns at failures were very similar in spite of different load levels. Points in common were;

(1) Main cracks extending as far as the neutral axsis of members are at a pitch of roughly d/2.
(2) Diagonal cracks causing shear failure in the end initiate at a reinforcing bar location approximately 1.5 d from the supporting point.

Regardless of the depth of "d", approximately same numbers of main cracks at shear failure appeared and that means crack widths are large when "d" is large comparison to that when "d" is small. In general, it is said that the shear strength of a beam without shear reinforcement is determined mainly by the interlocking action of aggregates, dowel action of axial reinforcing bars, and shear resistance of concrete at compression zones. Focusing on aggregate interlocking, crack width becomes large when "d" is large and the interlocking effect of aggregates will decrease, so that it may be considered that the shear strength will decrease when "d" is large.

Figure 12 shows the cracking pattern at the middle of the beam when d = 300 cm. At the center span, the principal cracks were formed first and followed by small cracks occurring at spacings as seen in a uni-axial tension test. This phnenomenon is quite similar to the pattern of internal cracks produced in concrete around deformed bars studied by Goto and Otsuka [11], and it is interesting that the microscopic cracking properties investigated by Goto and the macroscopic cracking properties in these large beams resemble well each other.

Figure 13 shows the cracking pattern at the shear span of a beam of d = 300 cm. In comparison between the A and Y sides, it is considered that the Y side shows a condition of shear failure, and the A side a condition immediately before failure, and as Kani [12] has stated, the mechanism as shown in Fig. 14 of ultimate failure at the bases of concrete teeth can be seen.

3.3 Loads and Reinforcing Bar Strain

The examples of the relationship between load and re-bar strain of d = 300 cm beam are shown in Fig. 15 and Fig. 16. Figure 15 is that of the midspan and Fig. 16 is for the section at 1.5 d inside from the supporting points. The calculated values in the figures are those obtained from the ordinary reinforced concrete calculation equation (hereafter RC calculations), but in the shear span, once a flexure shear crack is formed, a strain larger than that strain calculated by the conventional beam theory is produced. The method of computing the reinforcing bar strain for the acting moment by shifting toward lower moment section is called the moment shift method [13]. In this experiment, the strain corresponds to the values obtained from the RC calculation in which the moment shift of 1.0 d is considered.

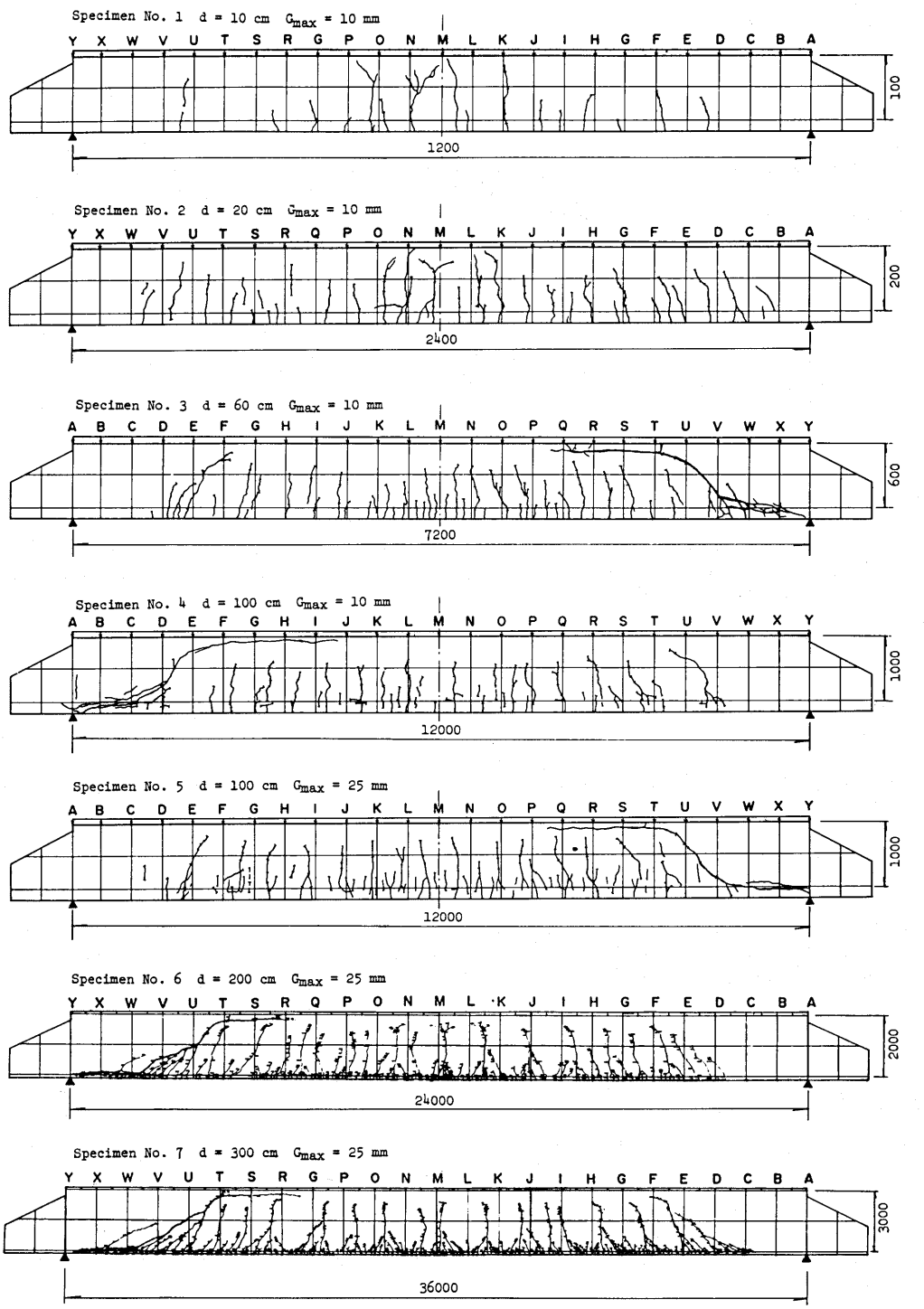

Fig. 11 Cracking patterns.

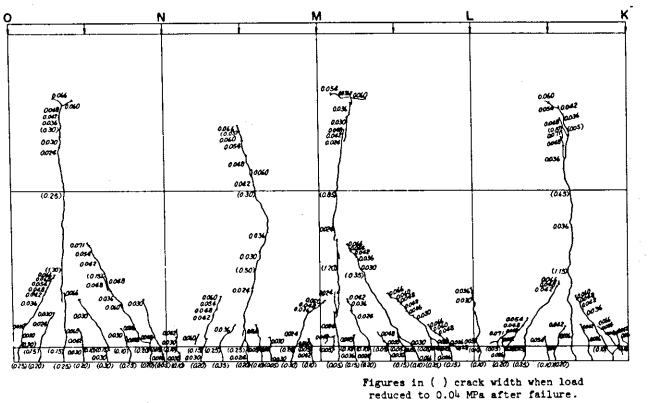

Fig. 12 Cracking pattern at midspan (Specimen No.7).

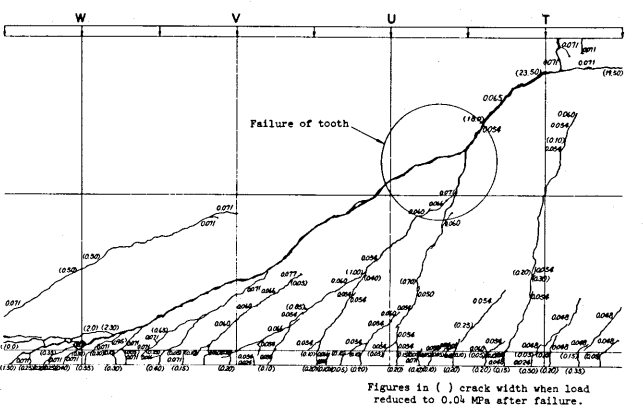

(Y side)

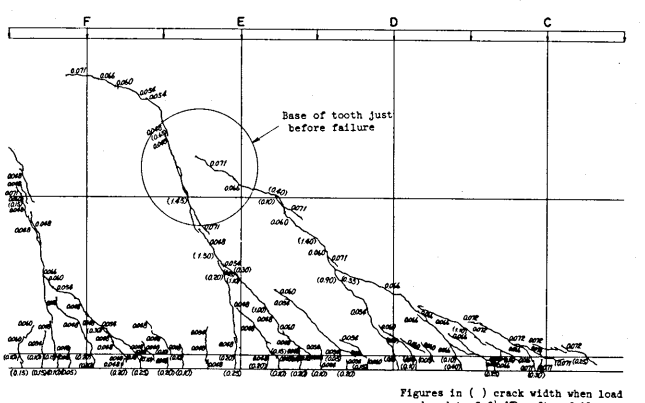

(A side)

Fig. 13 Cracking patterns at shear span (Specimen No.7).

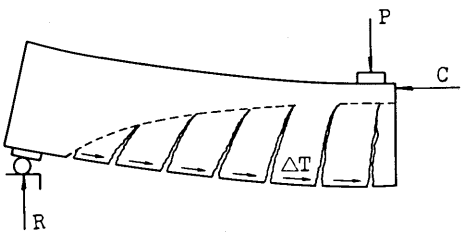

Fig. 14 Failure of tooth by Kani [12]

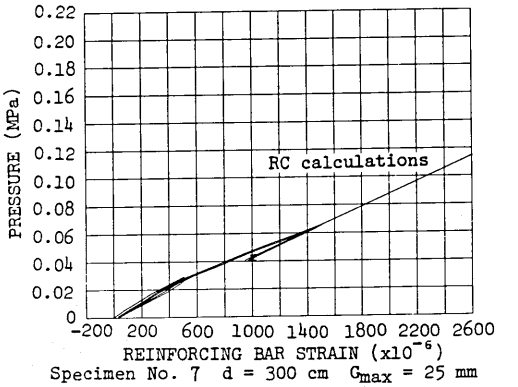

Fig. 15 Load and reinforcing bar strain at midspan (Specimen No.7)

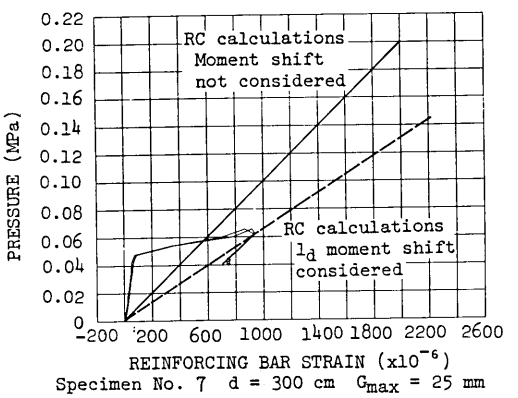

Fig. 16 Load and reinforcing bar strain at 1.5d inside of supporting point (Specimen No.7)

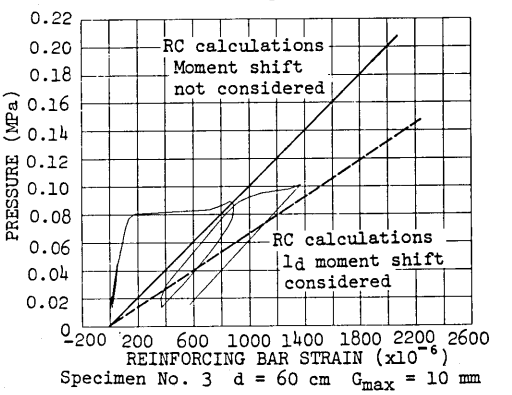

Fig. 17 Load and reinforcing bar strain at 1.5d inside of supporting point (Specimen No.3)

Figure 17 shows the reinforcing bar strains for d = 60 cm. Comparing the cases of d = 60 cm and 300 cm, the sudden increase of strain were observed in both cases and this phenomenon is considered due to the initiation of tensile cracks. The crack initiation load indicated by the inflection point was higher for the smaller member height. The actual flexural tensile strength of reinforced concrete beam specimen obtained from this inflection point is termed herein as the virtual flexural tensile strength f_b. On the other hand, the flexural tensile strength of plain concrete f_{bd} is obtained from the standard flexure test using 15 x 15 x 53 cm specimen, and this value can also be obtained by the relationship of $f_{bd} = 0.46\ f_c^{2/3}$, which is used in this study. The relation between the member height and the ratio of f_b/f_{bd} is shown Fig. 18. The figure shows the trend of f_b/f_{bd} to become smaller as the height of test specimen increases. It is conceivable that this phenomena is due to the size effect on the flexural tensile strength of concrete. Eventhough the possible effect due to bleeding is expected for the reversed loading direction on the specimens with d = 200 cm and 300 cm, no such effect is observed in the compressive strength test on core concrete specimens. The shear failure is initiated by formation of diagonal cracks or by the flexural failure at the base of concrete tooth as in Kani's theory. Both mechanisms are closely related to the flexural tensile strength. Therefore it is considered that the size effect on shear strength depends in part on the size effect of concrete flexural tensile strength itself.

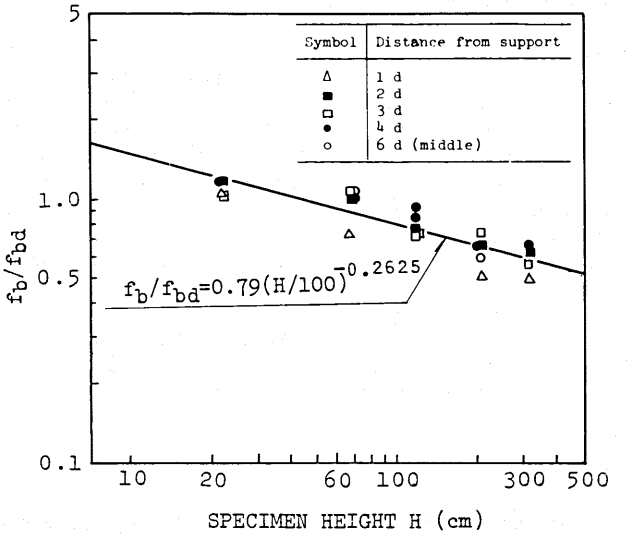

Fig. 18 Specimen height and flexural tensile strength.

3.4 Load and Deflection

Figure 19 shows the relation between load and deflection of a specimen with d = 300 cm. The calculated values in the figure are based on the equation proposed by Branson [14], but here, if calculations are made assuming that the flexural tensile strength f_{bd} of concrete is $f_{bd} = 0.46\ f_c^{2/3}$, there will be a discrepancy between calculated and experimental values. This can be attributed to the reason because the size effect exists in flexural tensile strength of concrete, and when calculations were made using the virtual flexural tensile strength f_b obtained from the load at which a reinforcing bar strain gauge sensed cracking, the relation between load and deflection agreed well for all specimens. Consequently, in case of calculating deflection in a large structure, it is considered necessary to take the size effect on flexural tensile strength of concrete into consideration.

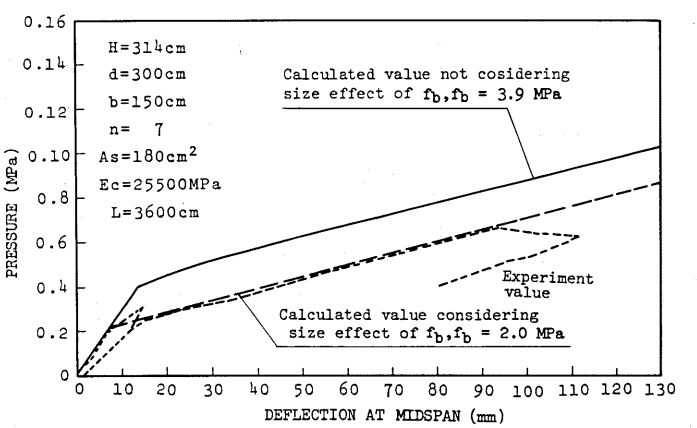

Fig. 19 Load and deflection at midspan (Specimen No.7).

3.5 Results of Bond Strength Tests

In the results of tensile strength tests on reinforcing bars (D16, D25) embedded in large specimens (d = 200, 300 cm), the strength at which the free-end slippage reached δ = 0.25 mm was defined to be the bond strength, and the results are reproduced in Figs. 20 and 21. A trend of bond strength decreasing at the upper part of the specimen was seen in tests using D16, but prominent differences were not recognizable in tests using D25. The large specimens all showed shear failures on the Y side, but bond strengths were higher on the Y side according to bond strength test results. This may seem at first glance to be contradictory, but Ikeda [15] has given a conceptual diagram of the strength of beams with bond strength as a parameter in connection with shear strength, which indicates the fact that high bond strength does not necessarily mean increased shear strength. At any rate, although bond and shear strength are closely related, there are many aspects which have not yet been clarified, and a clear-cut conclusion could not be drawn from the results of these tests.

3.6 Results of Concrete Core Strength Tests

The relation between the distance from the bottom of the specimen and concrete core strength is shown in Fig. 22. Concrete strength generally differs between upper and lower parts of a member due to the influence of bleeding, and it is

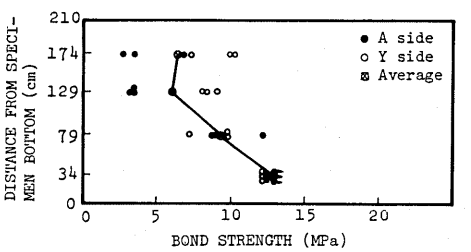

Fig. 20 D16 bond strength test results (Specimen No.6).

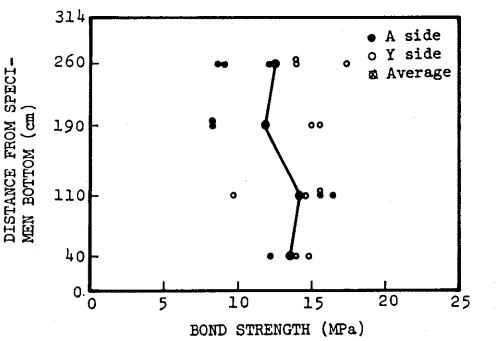

Fig. 21 D25 bond strength test results (Specimen No.7).

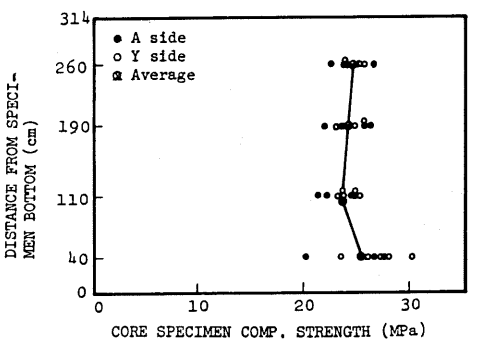

Fig. 22 Compressive strength test results of core concrete (Specimen No.7).

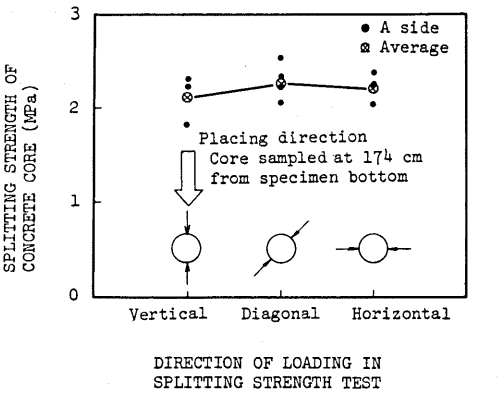

Fig. 23 Splitting tensile strength of core concrete according to direction of loading (Specimen No.6).

considered that strength at the upper part of the member is low, but in these experiments, since one lift of concrete placement was limited to about 80 cm, there was hardly any difference in strength seen in the direction of height. As shown in Fig. 23, splitting tensile strength tests were performed changing the direction of loading from the direction of concrete placement in a specimen of d = 200 cm, but differences in strength were not recognized.

4. CONCLUSIONS

The shear strength of a reinforced concrete beam without shear reinforcement has been found in experiments to be gradually reduced as beam depth increases, and this is generally called the size effect. The influences are partly adopted in various standards, but there has been no reports of experiments on the size effect on reinforced concrete beams of effective depth "d" being greater than 110 cm. Furthermore, there has been difficulty in assessing the shear capacity of large concrete members, which is composed largely of dead weight uniformly distributed, due to lack of the experimental data on the effect of distributed load. Accordingly, in this study the experiments under uniformly distributed loads were carried out on seven reinforced concrete beams of d = 10 to 300 cm without shear reinforcement, in order to examine whether the size effect on shear strength exists in beams mainly with "d" larger than 100 cm. The major results obtained were as follows:

(1) Size Effect on Shear Strength

According to the results of these experiments, shear strength gradually decreases as effective depth increases, similarly to the studies by Kani and Taylor. Moreover, it appears the CEB/FIP "Model Code for Concrete Structures," has not considered the size effect beyond the range of effective depth greater than 60 cm, but even for "d" greater than 100 cm, which had been outside the scope of past experiments, the size effect still exists. The size effect at d > 100 cm may be considered to be inversely proportional to the fourth root of effective depth.

(2) Cracking Pattern

Irrespective of the height of "d", the principal cracks at shear failure occurred at a pitch of d/2, and the number of cracks appeared were approximately the same. Consequently, the crack width will be larger when "d" is large, and it can be considered that the shear strength decreases when "d" is large, because the interlocking effect of aggregates will be reduced due to widening of cracks.

(3) Strain of Reinforcing Bar

The strain of reinforcing bar, when flexural shear cracks are formed, becomes larger than that calculated by the conventional beam theory. The method of computing the re-bar strain for the acting moment shifted toward the lower moment section is called the moment shift method. In this experiment, the re-bar strain corresponds to the values obtained from the RC calculation in which the moment shift of 1.0 d is considered.

The virtual flexural tensile strength f_b obtained from the load at which the reinforcing bar strain gauge sensed crack initiation is lower for specimens with greater height "H", and it is thought the size effect on shear strength of a beam without shear reinforcement is due in part to the size effect of concrete flexural tensile strength itself.

(4) Load and Deflection

The experimental and analytical values of load-deflection were compared, and the both values showed better agreement when the virtual flexural tensile strength, which incorporates the size effect, was used for the analysis than when the ordinary flexural tensile strength was used. Consequently, for calculating deflection of a large structure, it is considered necessary to take the size effect on flexural tensile strength of concrete into account.

ACKNOWLEDGEMENTS

The authors sincerely thank Prof. Shoji Ikeda, Department of Civil Engineering, Yokohama National University, Prof. Hajime Okamura, Department of Civil Engineering, University of Tokyo, and Dr. Yukio Aoyagi, the head of material mechanics section at Civil Engineering Laboratory, Central Research Institute of Electric Power Industry for valuable advice given throughout the study.

References

[1] Kani, G. N. J.: "How Safe Are Our Large Reinforced Concrete Beams?," Journal of the American Concrete Institute, No. 64-12, March 1967
[2] Kennedy, R. P.: "A Statistical Analysis of the Shear Strength of Reinforced Concrete Beams," Ph.d. Dissertation to Stanford University, 1967
[3] Taylor, H. P. J: "Shear Strength of Large Beams," Journal of Structural Division, Proceedings of the American Society of Civil Engineers, November 1972.
[4] CEB/FIP: "Model Code for Concrete Structures," 1978.
[5] Japan Society of Civil Engineers: "Limit State Design of Concrete Structures (Proposal)," Concrete Library, No. 52, November 1983 (in Japanese).
[6] Higai, T.: "Behavior of Reinforced Concrete Members (Part 4)," Concrete Library, No. 34, JSCE, August 1972 (in Japanese).
[7] Kani, G. N. J.: "Basic Facts Concerning Shear Failure," Journal of ACI, June 1966.
[8] Murayama, Y. Noda, S., and Iwaki, R.: "Small-Scale Model Test by Using 3-mm Diameter Deformed-Bar," Proceedings of Japan Concrete Institute, 4th Conference, 1982 (in Japanese).
[9] JSCE: "Standard Specifications for Unreinforced and Reinforced Concrete," Instituted 1974 (1980 Edition) (in Japanese).
[10] Okamura, H., and Higai, T.: "Proposed Design Equation for Shear Strength of Reinforced Concrete Beams without Web Reinforcement," Proc. of JSCE, No. 300, August 1980.
[11] Goto, Y., and Otsuka, K.: "Experimental Studies on Cracks Formed in Concrete Around Deformed Tension Bars," Proc. of JSCE, No. 294, February 1980 (in Japanese).
[12] Kani, G. N. J.: "The Riddle of Shear Failure and Its Solution," Journal of ACI, April 1964.
[13] Ikeda, S.: "Standard Specifications for Unreinforced and Reinforced Concrete - A Partial Amendment of the Design Code," Concrete Library, No. 46, JSCE, April 1980 (in Japanese).
[14] Branson, D. E.: "Instantaneous and Time-Dependent Deflections of Simple and Continuous Reinforced Concrete Beams," Report No. 7, Alabama Highway Research Report, U.S. Bureau of Public Roads, August 1963.
[15] Ikeda, S., and Uji, K.: "Studies on the Effect of Bond on the Shear Behavior of Reinforced Concrete Beams," Proc. of JSCE, No. 293, January 1980 (in Japanese).